

---

This is an electronic reprint of the original article.  
This reprint may differ from the original in pagination and typographic detail.

Li, Fang; Suominen, Mikko; Kujala, Pentti

## Ship performance in ice channels narrower than ship beam

*Published in:*  
Ocean Engineering

*DOI:*  
[10.1016/j.oceaneng.2021.109922](https://doi.org/10.1016/j.oceaneng.2021.109922)

Published: 15/11/2021

*Document Version*  
Publisher's PDF, also known as Version of record

*Published under the following license:*  
CC BY

*Please cite the original version:*  
Li, F., Suominen, M., & Kujala, P. (2021). Ship performance in ice channels narrower than ship beam: Model test and numerical investigation. *Ocean Engineering*, 240, Article 109922.  
<https://doi.org/10.1016/j.oceaneng.2021.109922>

---

This material is protected by copyright and other intellectual property rights, and duplication or sale of all or part of any of the repository collections is not permitted, except that material may be duplicated by you for your research use or educational purposes in electronic or print form. You must obtain permission for any other use. Electronic or print copies may not be offered, whether for sale or otherwise to anyone who is not an authorised user.



# Ship performance in ice channels narrower than ship beam: Model test and numerical investigation

Fang Li<sup>\*</sup>, Mikko Suominen, Pentti Kujala

Department of Mechanical Engineering, Aalto University, FI-00076, AALTO, Finland

## ARTICLE INFO

### Keywords:

Ship performance in ice  
Narrow ice channel  
Ship resistance  
Level ice  
Arctic ships  
H-v curve

## ABSTRACT

During escort and convoy operations, an icebreaker opens a channel while the escorted or convoyed ships follow the path along the channel. If the assisted ship is wider than the channel which the icebreaker creates, the created channel cannot fit the assisted ship. Thus, the assisted ship has to break some ice by itself. This is herein referred to as navigation in 'narrow ice channel'. The performance of ships in narrow ice channel is investigated here. For this aim, model-scale test of a ship going through ice channels with different widths and ice thicknesses is firstly conducted. After that, numerical simulation of the model test scenarios is implemented with an in-house simulation program dedicated for ship operation in ice. The simulation correctly captured the main features of ship resistance change as a function of channel width, which indicates its validity as a simulation tool. Subsequently, numerical simulations are implemented with several other ships in order to gain general insights into performance of ships in narrow ice channel. Focus is given to the influence of channel width on ships' encountered resistance and attainable speed in ice. The general findings through these simulations are useful for decision making tools.

## 1. Introduction

Merchant ships in ice-covers areas often need assistance from dedicated icebreakers in order to go through ice fields where the ice condition is too difficult for an independent operation. Escort and convoy are typical operations, during which the assisted ship follows the lead of an icebreaker which breaks ice and creates a channel for the following ship. It is typically preferred that the width of the channel is larger than that of the assisted ship to avoid a contact between the assisted ship and the edge of the channel. Motivated by this, icebreakers are often designed with a large breadth in order to break wide ice channels. An example of such motivation is the oblique icebreaker *Baltika* (Hovilainen et al., 2014), which can operate obliquely and breaks a much wider channel than its own breadth. However, if the assisted ship is wider than the broken channel, a part of the hull is in contact with the ice sheet at the channel edge and has to break the ice in order to proceed. This creates more resistance than the case with wider channel. Thus, the attainable speed of the assisted ship decreases. Such scenario is herein referred to as *ships in narrow ice channel*. Such cases are known to occur on the Northern Baltic Sea during wintertime and are also relevant for large size ships along the Northern Sea Route (NSR) that have been built

with increasing numbers during recent years (Sazonov, 2011; Dobrodeev et al., 2018).

In a narrow channel, naturally, the resistance as well as ship speed are functions of the channel width. Quantitative calculation methods for such operation are rare in the literature. Dobrodeev et al. (2018) mentioned that the resistance can be analytically calculated using Innov method, but the formulations were not given. The methodology which Dobrodeev et al. (2018) adopts is to derive the resistance in narrow channels based on the theoretical basis of an existing formula for level ice. Such methodology may also be possible to be realized based on other resistance formulae, e.g. Lindqvist (1989), Kämäräinen (1993). In addition to analytical approach, it is also possible to simulate ships in narrow ice channel with a numerical simulation program, such as Lubbad and Løset (2011), Su et al. (2010), Zhou et al. (2020). However, there has been no attempt to apply these to simulate ships in narrow channels.

This paper investigates ships' performance in narrow ice channel, in terms of encountered resistance and attainable speed. The initiation of this work comes from the need to evaluate ship performance in narrow channels in the context of a system-level decision making tool for the Finnish-Swedish winter navigation system (Lindeberg et al., 2018). The

<sup>\*</sup> Corresponding author. Postal address: Aalto University, School of Engineering, Marine Technology, P.O. Box 15300, 00076, Aalto, Finland.  
E-mail address: [fang.li@aalto.fi](mailto:fang.li@aalto.fi) (F. Li).

research questions are: how changes in the channel width alter the ice resistance and attainable speed of different ships? The focus is on the effectiveness of escort/convoy, i.e. the resistance reduction and speed increase as a function of channel width with respect to the resistance and attainable speed in level ice. Within this scope, the relative change of resistance and speed are in focus, while their absolute magnitudes are of less concern.

The investigation is carried out in two parts. In the first part, model-scale tests are conducted at Aalto Ice Tank with a ship model Infuture that was designed within an EU-project INFUTURE. The test program covers the ship going through level ice, open ice channel and narrow ice channel with different channel widths. The program enables the determination of resistance change as a function of channel width from totally open channel (the channel width is larger than the ship breadth) to totally closed channel (level ice). Two different ice thicknesses are used. The second part implements numerical simulation to further investigate the phenomenon and to form generalized conclusions which also hold for other ships. The simulation is carried out with the in-house simulation software ASOIS (Aalto Ship Operation in Ice Simulator), which is developed by Li et al. (2020a) based on extensive ship-ice interaction modelling (Li et al., 2019a, 2020b, 2019a). The simulation program is first benchmarked with the model-scale test results by setting up and computing the same scenarios in the simulator. After the validity of the simulation program is confirmed through the comparison with model test results, similar simulation scenarios are carried out with different ships. This paper then attempts to attain general conclusions about the effect of channel width on ships' encountered resistance and attainable speed, i.e. the so-called h-v curves. This offers general insights and provide quantitative tools to evaluate ships' performance in narrow ice channel.

## 2. Methods of investigation

### 2.1. Definitions

Ice resistance in a narrow channel comes from two parts: i) displacing broken ice pieces in the channel and ii) breaking and displacing the level ice sheet at the channel edge. For a ship following an icebreaker, the amount of ice in the ice channel created by the icebreaker mainly depends on the capability of the icebreaker to clear the broken ice sideways. Such an ice channel differs from the brash ice channel which usually has higher concentration and ice column thickness as well as smaller and more rounded ice pieces. As pointed out by Huang et al. (2021a), modern icebreakers can be designed with certain techniques to push the broken ice under the ice sheets, thus clearing the channel. The amount of ice pieces left in a channel is then rather small,

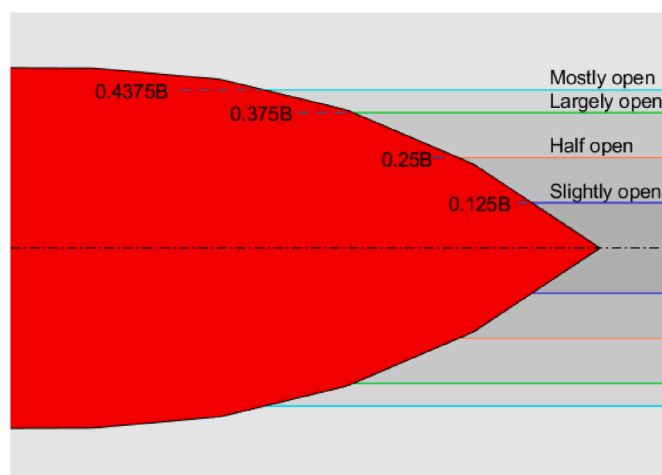


Fig. 1. Definition of channel width extent.

sometimes even resulting in open water channel (see Fig. 1b of Huang et al. (2021a)). Therefore, it can be reasonably assumed that the resistance in a narrow channel mainly comes from ice breaking and subsequent processes from the interaction with the ice sheet at channel edges. Following this, the model-scale test and numerical simulation are set up with a narrow open water channel. For the convenience of later presentation, the non-dimensional channel width, denoted as  $\gamma$ , is defined as per

$$\gamma = \min\left(\frac{w}{B}, 1\right) \quad (1)$$

where  $w$  is the channel width and  $B$  the ship breadth. With  $\gamma = 0$ , the channel edges are connected together representing level ice field; with  $\gamma = 1$ , the channel is wider than the ship representing open ice channel; with  $0 < \gamma < 1$ , a narrow ice channel is represented.

In addition, we denote  $r$  as the non-dimensional ice resistance normalized by the level ice resistance, as per

$$r = \frac{R}{R_{level}} \quad (2)$$

where  $R$  is the ice resistance in a narrow channel and  $R_{level}$  is the resistance in level ice with the same ice thickness. Specifically, we denote  $r_\gamma$  as the non-dimensional ice resistance when the channel width is  $\gamma$ .  $r_\gamma$  can be seen as an index of the escort/convoy effectiveness which tells the proportion of remaining resistance comparing to that in level ice.

For the convenience of describing the extent of a channel width in comparison to the ship width, five levels of channel width are defined. A channel with  $\gamma$  around 1/4 is referred to as *slightly open channel*,  $\gamma$  around 1/2 as *half open channel*,  $\gamma$  around 3/4 as *largely open channel*,  $\gamma$  around 7/8 as *mostly open channel* and  $\gamma$  equaling 1 as *open channel*. This is schematically shown in Fig. 1. Further, we define the *escort performance* of a ship as the resistance reduction and speed increment in a narrow channel as a function of relative channel width. A ship is judged to have better escort performance if the remaining resistance  $r_\gamma$  is small in comparison to other ships. In reality, it is rather unlikely that an escorted ship is twice as wide as the assisting icebreaker. Nonetheless, ships may still encounter very narrow channel if the ice sheets are driven by the wind and thereby closing behind an icebreaker (Li et al., 2019b).

It is commonly known that the hull angles have a major effect on the resistance a ship encounters. Here we denote  $\varphi$  as the flare angle of the hull at any location, which is the angle between the normal vector and vertical direction as per Fig. 2. Following this and referring to Fig. 1, we define  $\varphi_1$ ,  $\varphi_2$ ,  $\varphi_3$  and  $\varphi_4$  as the mean flare angle along the hull between the centerline and 0.125B, 0.125B and 0.25B, 0.25B and 0.375B, 0.375B and 0.5B (i.e. half breadth), respectively for later use. These are the mean flare angles of the four quarters of ship width.

### 2.2. Model-scale test

The model tests were carried out at Aalto Ice Tank during spring 2021 as a part of INFUTURE project which focuses on inland waterway vessels. The model ship Infuture is a double-acting general cargo vessel which breaks ice astern. Basic information of the vessel is listed in Table 1. The ship is designed to break 0.6m level ice with speed of 2knots astern. The ice class is IAS according to Finnish-Swedish ice class rules.

Within the project context, relatively strong ice has been used following the measurement campaign on the Finnish Saimaa Lake (Suominen et al., 2021). Fine-grained ethanol doped model-scale ice sheet ice was produced by spraying layers of fine mist over a period of several hours. The structure of ice and the added dopant enable the adjustment of the mechanical properties of ice to the desired level for model-scale tests. The ice channels were cut with a drill installed on the carriage. This allowed an accurate control of the desired widths. The cut ice was then cleared from the channel leaving a narrow open water channel. Following the described procedure, channels with five different

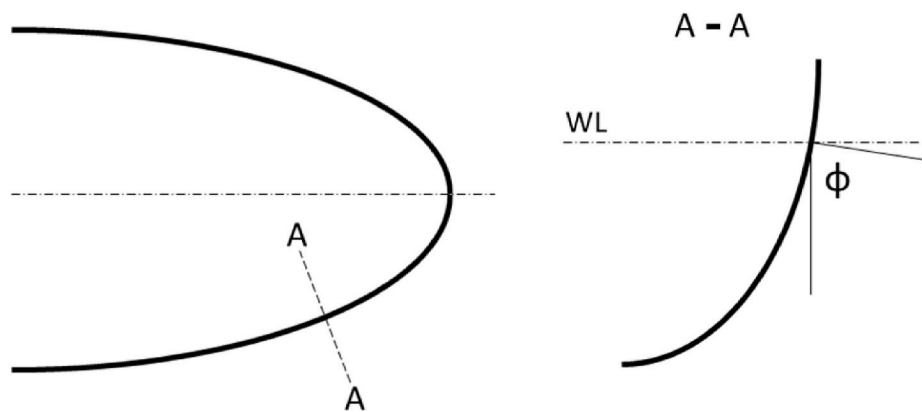


Fig. 2. Flare angle definition.

Table 1  
Ship particulars.

	Full-scale	Model-scale	Unit
Length overall	92.5	5.50	m
Breadth	12.6	0.75	m
Depth	8	0.48	m
Draught	4.45	0.26	m
Displacement	4053	0.852	t
Open water service speed	5.92	1.44	m/s
Full power	1678	0.09	kW

widths were prepared, with  $\gamma$  being 0, 0.25, 0.5, 0.75 and 1, which represent level ice, slightly open channel, half open channel, largely open channel and open channel.

The model-scale tests were conducted as towed resistance tests. For each test, the model ship was placed in the beginning of the prepared channel and the centerline of the model ship was aligned with the centerline of the channel. Fig. 3 presents a photo of a half open channel with the model ship at the starting position. The model ship was connected to the carriage by the towing cable. The towing force was measured with a 500N load sensor between the pulling cable and the attachment to the carriage. Shackle-shackle connection between the load sensor and the model prevented the possible moments induced by the connection. A counter weight was applied to damp the possible surging motions during the tests. Furthermore, the heading of the model was kept aligned with the channel by restricting the sway and yaw motions with two guiding posts one at the bow and one at the stern, see the blue frame in Fig. 3.

Ice properties including elastic modulus, thickness, flexural strength and compressive strength are measured in-situ following ITTC recommendations (ITTC, 2017). The thickness and strength properties were measured at different locations close to the testing locations with three

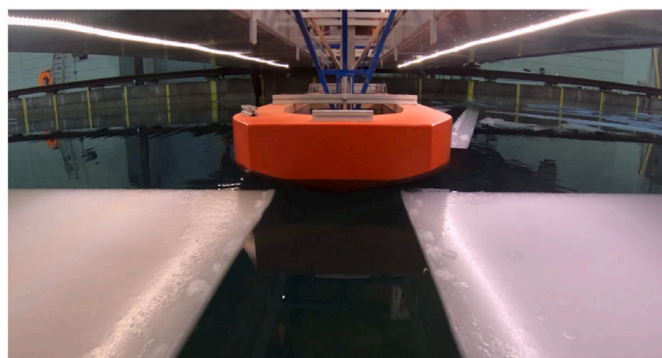


Fig. 3. Half open channel made for the test. Model at the starting position.

tests at each location. The strength properties are summarized in Table 2 together with the test programme. Overall, ice thickness varies very little between different locations, while strength properties vary more. The actual towing test were carried out about three to four hours after the mechanical properties were measured. Due to this time interval, some deviations may be expected between the actual strength and measured strength. However, the deviation is expected to be minor as the temperature was kept at preservation level.

The test program is listed in Table 2. In total, two ice sheets were created separately on 25th and 30th March, with different thicknesses corresponding to 36 cm and 61 cm in full scale. The flexural strength corresponds to about 800 kPa and 1 MPa in full-scale since the background project focuses on freshwater ice. The towing speeds are kept at 0.488 m/s, which corresponds to 2 m/s in full scale. The scaling rules are presented in Table 3, which follows standard procedure with Cauchy and Froude similarities (ITTC, 2017).

The dynamic friction coefficient is measure ex-situ on the model surface. The model was turned on its side and the testing area on the hull was surrounded with aluminum frames. The testing area was covered with a thin layer of basin water to secure the wet contact. An ice sample was extracted from the model ice sheet and placed top surface against the model hull. A deadweight of 2 kg and a wooden plate were placed above the ice sample after weighing. The system was moved back and forth approximately a length of 1.5 m with a step-motor system. The required force was measured with a load sensor to determine the friction coefficient. Three frictional tests are conducted following this procedure, which gives average friction coefficient 0.085 with small variation.

2.3. Numerical simulation

The simulation programme ASOIS is developed by Li et al. (2020a) based on the combination of several submodels to model different

Table 2  
Test program and measured ice properties.

Test No.	Speed m/s	Channel width	E (MPa)	$\sigma_f$ (kPa)	$\sigma_c$ (kPa)	h (mm)
1.1	0.488	0.375m	156.3	40.5	31.4	22
				35.349.2		
1.2	0.488	0.187m		49.2	35.6	21
1.3	0.488	0.562m		57.4	37.5	20
1.4	0.488	0m (level ice)		50.1	42.4	22
1.5	0.488	0.8m (open water)	Irrelevant			
2.1	0.488	0.375m	234.7	52.9	48.4	36
				63.052.1		
2.2	0.488	0.187m		52.1	59.5	36
2.3	0.488	0.562m		68.8	79.5	38
2.4	0.488	0m (level ice)		77.6	70.1	36

**Table 3**  
Scaling rules.

Parameters	Scaling factor
$B$	$\lambda$
$w$	$\lambda$
$v$	$\lambda^{1/2}$
$E/\sigma_f/\sigma_c$	$\lambda$
$h$	$\lambda$
$R$	$\lambda^3$

icebreaking processes as well as ship thrust and rudder force. Fig. 4 illustrates the structure of ASOIS where the source of each submodel is listed. The simulation programme is the assembly of these submodels, including propeller thrust model according to Li et al. (2018), rudder force model according to Molland and Turnock (2007), hydrodynamic force model according to Matusiak (2017), as well as several models within the ice force part, elaborated below.

The algorithm starts with detection of contact area between ship and ice polygons, based on which the crushing force is calculated via the compressive strength of ice. The algorithm then extract the feature of the contact area and use models described in Li et al. (2019a, 2020b) to compute the maximum stress in the ice sheet. Hydrodynamic effect on ice bending is taken into account with a method described in Li et al. (2020a), which is based on Tan et al. (2014) and Wang (2001). The algorithm then checks whether bending failure happens by comparing the maximum stress with flexural strength, and updates the ice polygon accordingly if bending failure occurs. After an ice piece is broken off from the intact ice sheet, rotation of the ice piece against ship hull is simulated according to the model of Li et al. (2020a), until the ice piece becomes parallel to the hull. The subsequential submerging process is not simulated, but instead analytically calculated using Lindqvist (1989) formula. A thorough description of each submodel is omitted here due to its extensiveness. The readers are referred to Li et al. (2020a) for more information related to the establishment of this programme. The simulation is relatively fast as it requires no material level computations such as Finite Element Analysis. A simulation of towing test can be finished typically within hours with normal PC.

The simulation programme does not contain tunable parameters so there is little simulation uncertainty related to subjective choice of parameters, except for those associated with the input parameters. Inputs of the simulation programme contain ice properties including flexural strength, compressive strength and elastic modulus, ship water line geometry and associated hull angles, as well as simulation parameters such as ship speed and ice thickness. The programme has been benchmarked with full-scale measurement data obtained with ship S.A.

Agulhas II on the Baltic Sea (Li et al., 2020a).

To simulate ships going through narrow ice channel, two level ice sheets are set up in the programme with a channel of width  $w$  in between, schematically shown in Fig. 5. Small perturbations are introduced to the channel edge to mimic the reality, so that the local channel width varies slightly while the global mean width is kept as  $w$ . The breaking of intact ice sheet and rotation of ice pieces after breaking can be numerically computed by the programme, similar as ships in level ice field. Since the programme adopts the formula of Lindqvist (1989) to calculate the submersion process instead of numerically simulating the movement of ice pieces generated by ice breaking process, to enable submersion resistance calculation in a narrow channel, the submersion force calculated via Lindqvist formula is linearly scaled with a factor  $1 - \gamma$ , which is the non-dimensional channel edge ice sheet width project to ship breadth. The total ice resistance,  $R$  is then calculated as

$$R = R_{b,simulation} + R_{r,simulation} + (1 - \gamma)R_{s,Lindqvist} \tag{3}$$

where  $R_{b,simulation}$  and  $R_{r,simulation}$  are ice breaking and rotation resistance which are numerically computed in a narrow channel;  $R_{s,Lindqvist}$  the submersion resistance formula derived by Lindqvist (1989) for level ice. Such formulation ensures that when  $\gamma = 1$ , the resistance equals open channel resistance while when  $\gamma = 0$  it converges to level ice resistance.

In addition to ship model Infuture, simulations will be carried out with ten other ships in order to attain general conclusions on ship performance in narrow ice channel. This includes ships Envik, Kemira, Solano, Tebostar, Uikku, Aranda, Agulhas II, R-class icebreaker, Polar-class icebreaker and a general cargo vessel (GCV). The main particulars of these ships are summarized in Table 4, with sketches of the waterlines showing in Fig. 6. These ships are selected because of our access to their line drawings, which is needed for the implementation of the numerical programme. The ships selected cover not only merchant vessels; this is for research purpose to derive general conclusions. The lengths of the selected ships range from 51m to 156m and block coefficient from 0.56 to 0.80. Since the aim is to investigate the influence of channel width on ships' icebreaking capability, only ships which are capable of independent navigation in level ice are considered in the selection, while ships which are not designed to break ice are not within scope.

### 3. Results of model test and numerical simulation

#### 3.1. Results with ship infuture

##### 3.1.1. Model test

The resistance scaled from the mean towing forces during the tests are summarized in Fig. 7, plotted as functions of channel width. The

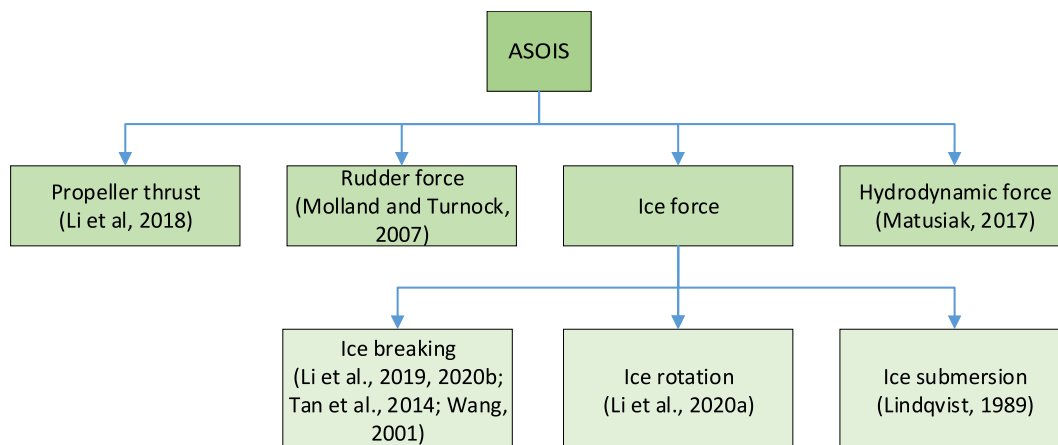


Fig. 4. Structure of ASOIS and sources of submodels.

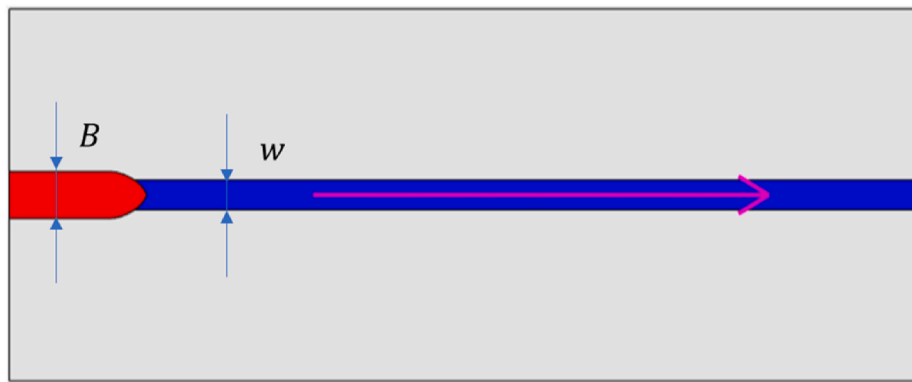


Fig. 5. Illustration of simulation setup with a ship in half open channel.

Table 4

List of sample ships to be used in the simulations.

Ship name	Length (m)	Breadth (m)	Draught (m)	Block coefficient
Envik	96	16.5	5.2	0.68
Kemira	105	17	8.1	0.74
Solano	116	21	6.2	0.69
Tebostar	106	17.6	6.6	0.63
Uikku	156	21.5	9.5	0.71
Agulhas II	126	22	7.65	0.64
R-class icebreaker	93	19.2	7.2	0.63
Polar-class icebreaker	107.3	23.8	9.1	0.57
General cargo vessel	149.3	24.6	9.4	0.80
Aranda	51.2	13.8	4.6	0.56

mean ice thicknesses of the two ice sheets are 21.25 mm and 36.5 mm, which correspond to scaled ice thicknesses of 36 cm and 61 cm. Resistance from water has been excluded from the forces by subtracting the measured open channel resistance from the measured towing force. The relative resistance changes are plotted in Fig. 8, where the resistance has been normalized by the corresponding level ice resistance. The resistance reduces as channel width increases. The largest resistance reduction comes from the opening of channel from  $\gamma$  being 0 to 0.25, in which case the stem loses contact with ice. This reduction accounts for 35% and 41% of the level ice resistance in the 36 cm and 61 cm ice sheets respectively. The second largest resistance reduction comes from the opening of channel from three quarters to one, in which case the shoulder loses contact with ice. This reduction accounts for 27% and 23% of the level ice resistance in the 36 cm and 61 cm ice sheets respectively. The resistance changes from slightly open channel to half open channel and from half open channel to largely opened channel are the smallest, altogether accounting for 38% and 35% of the level ice resistance in the 36 cm and 61 cm ice sheets respectively. The thickness seems to have rather small influence on the relative magnitude of narrow channel resistance with different channel width.

### 3.1.2. Simulation

The simulations are conducted in full scale with input parameters scaled from measurements. The same scenarios as in the model tests are set up in the simulation programme. The mean of measured thickness and strengths in each ice sheet are used. All the input parameters have been either measured or controlled, thus no input parameters are assumed. The obtained resistance from the simulations are therefore definite since the results do not depend on any assumed parameters. Fig. 9 presents an example of the simulation which shows the ship going through a half open channel with 36 cm ice. Note that the simulation program only visualizes the ship and intact ice sheet, while the broken ice pieces are not visualized although their motions are tracked.

The simulation results are plotted in Figs. 7 and 8 together with the measurement results. Overall, the deviations seem to be larger in the 36 cm ice sheet comparing to the cases in the 61 cm ice sheet. The level ice resistance is underestimated by 16.7% and 14.8% in the 36 cm and 61 cm ice sheets respectively, which is acceptable. The simulation results show similar relative importance of the four quarters as demonstrated by the measurement, i.e. the opening of the first quarter of the channel leads to greatest resistance reduction and the last quarter leads to the second largest reduction. Since the aim of this paper is to investigate the influence of channel width on ships' encountered resistance, the relative magnitudes shown in Fig. 8 are of more importance comparing to the absolute values in Fig. 7. The comparison between the measurement and simulation indicates that the simulation results well captures the change of resistance with different channel width. Better agreement is shown with the 61 cm case, where the scatter of simulation locates rather close to that obtained from measurement. These provide the ground for the use of the simulation programme to investigate the performance change of other ships in narrow ice channel.

### 3.2. Simulation results with sample ships

Simulations of other ships listed in Table 4 are carried out with full-scale sea ice conditions, with compressive strength of 1 MPa, flexural strength of 500 kPa and elastic modulus of 5 GPa. As the first step, we will test whether ice thickness and ship speed have major influence on

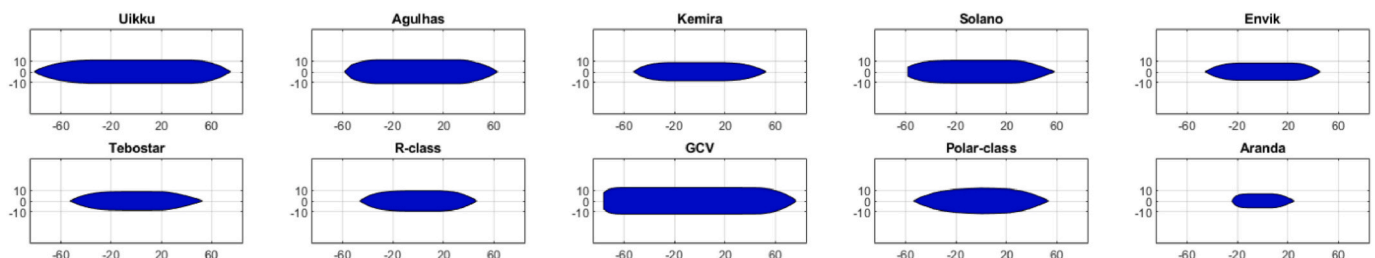


Fig. 6. Sketch of the waterlines of sample ships.

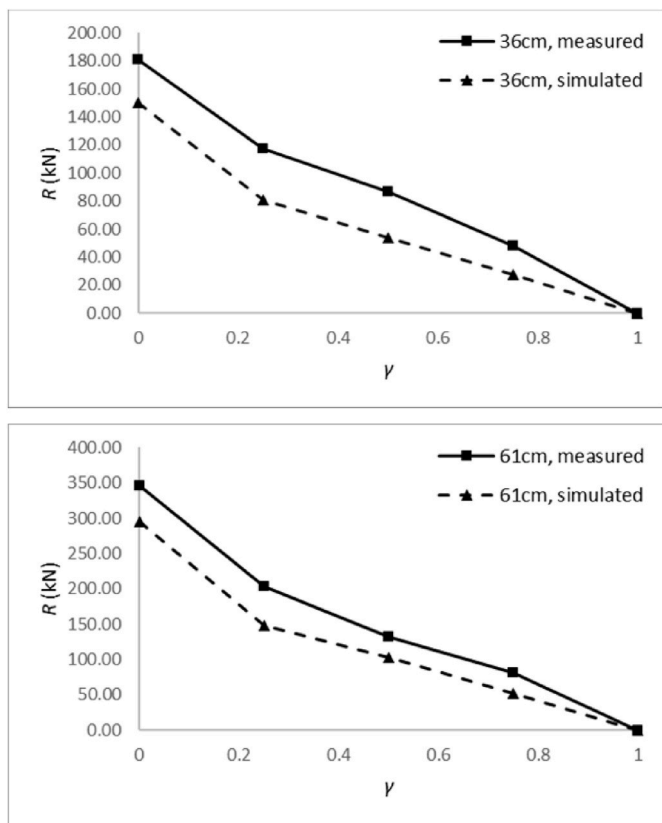


Fig. 7. Ice resistance scaled from the measurement and simulated with ASOIS.

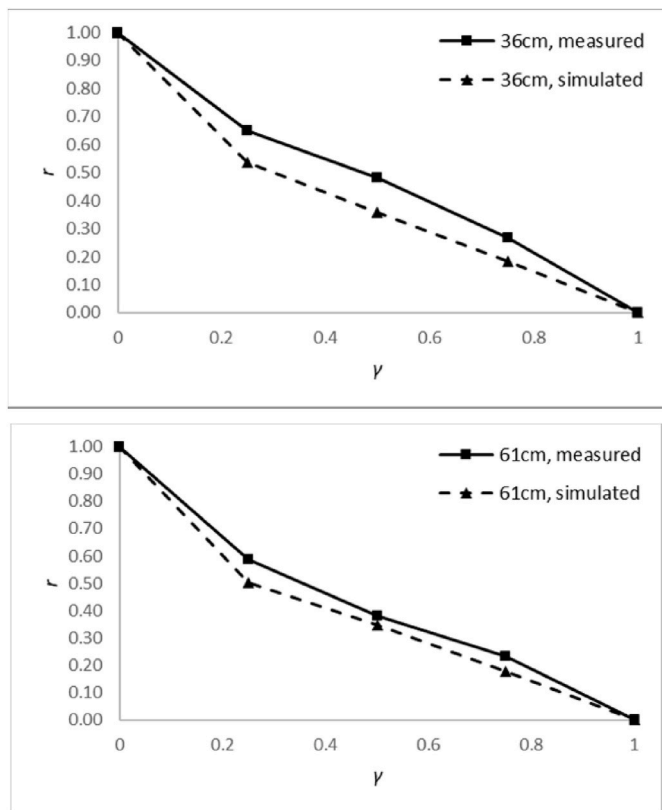


Fig. 8. Relative ice resistance from the measurement and simulated with ASOIS.

the normalized resistance-channel width curves. This is demonstrated through the simulation of ship Uikku in three thickness-speed combinations, including 0.3m and 2 m/s, 0.6m and 2 m/s, as well as 0.3m and 4 m/s. The results of normalized resistance are plotted in Fig. 10 as functions of channel widths. It can be seen from this figure that the variation in thickness has little influence on the normalized resistance-channel width curve. A larger speed seems to increase the resistance proportion around the stem because of hydrodynamic effect on ice bending, but the influence is mild. Therefore, without loss of generality, the later simulations are carried out with ice thickness of 0.3m and speed of 2 m/s.

Fig. 11 summarizes the simulation results of the ten sample ships, plotted in terms of non-dimensional resistance,  $r$ , as a function of non-dimensional channel width,  $\gamma$ . It is found that in some cases even with largely open channel, the remaining ice resistance is still very high. Thus, in addition to channel width 0.25B, 0.5B and 0.75B, additional simulations are carried out in mostly open channel with a channel width of 0.875B. A channel width of 0.875B represents ships travelling in ice channels which are only slightly narrower than ship widths.

The trends of the resistance-channel width curves clearly differ between the sample ships. Some ships have relatively linear curves where the resistance reductions vary little every time the channel is opened a quarter more, such as Agulhas II and Polar-class icebreaker, while some ships have significant remaining resistance up to 80% although the channel is largely open, e.g. Kemira and Envik. The common feature with all the ships in the simulation results is that the largest resistance reduction occurs either in the first or the last quarter ( $\gamma$  from 0 to 0.25 or 0.75 to 1), while the resistance reductions in the middle two quarters ( $\gamma$  from 0.25 to 0.5 and from 0.5 to 0.75) are usually smaller. The same has been seen in the model test results presented in Section 3.1.1.

Fig. 11 indicates that in some cases, opening of the channel may even lead to increase of resistance, e.g. Kemira, Envik and Tebostar. It is worthwhile to look into the reason behind this observation. Fig. 12 presents the ice breaking resistance distribution along the hull of Kemira in a half open channel and a largely open channel, where the height of a bar represents the resistance on a small width interval. As indicated by the resistance distribution charts, resistance at a small width interval close to full breadth dominates the total remaining resistance. This resistance section becomes larger in largely open channel, which leads to higher resistance. The cause of this is that the ship hull is more inclined at the edge of half open channel, which enables breaking of ice by bending. Ice pieces are broken off the ice sheet, which results in less ship-ice contact in the shoulder area. Nonetheless, the ship flare angle at the edge of largely open channel is so large (about 70°) that bending failure becomes rarer and the ice fails mainly through crushing at the shoulder area, thereby resulting in higher resistance. As will be shown in Fig. 14, these three ships (Kemira, Envik and Tebostar) have the largest flare angle at the shoulder area, which are more prone to shoulder crushing.

To investigate the reasons behind the differences in the resistance-channel width curves, the non-dimensional resistance reductions are plotted in Fig. 13 as bar charts. The height of a bar represents the resistance reduction when the channel opens further by a quarter. It is known that ship resistance is largely determined by hull angles. Therefore, the mean flare angles  $\varphi$ , of each quarter of ship width are plotted as scatter points in the same figure via their tangent values. The mean flare angles in the four quarters have been denoted by  $\varphi_1$ ,  $\varphi_2$ ,  $\varphi_3$  and  $\varphi_4$  as defined in Section 2.1. The  $\varphi$  angles of the ten ships are further summarized in Fig. 14 for the easy comparison between ships. Tangent values and scales are adopted because it determines the ratio between the force components in horizontal plane and vertical direction, which are the forces leading to resistance and leading to ice bending failure. The magnitudes of resistance reduction in each quarter becomes explainable with the assistance of mean flare angles, classified below as three types.

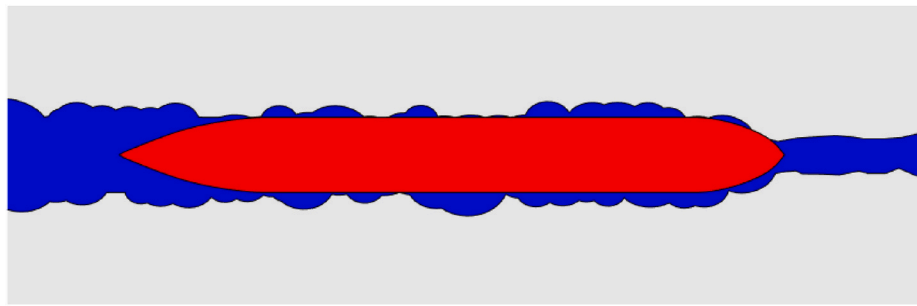


Fig. 9. Visualization of the simulation with Infuture model in half open channel.

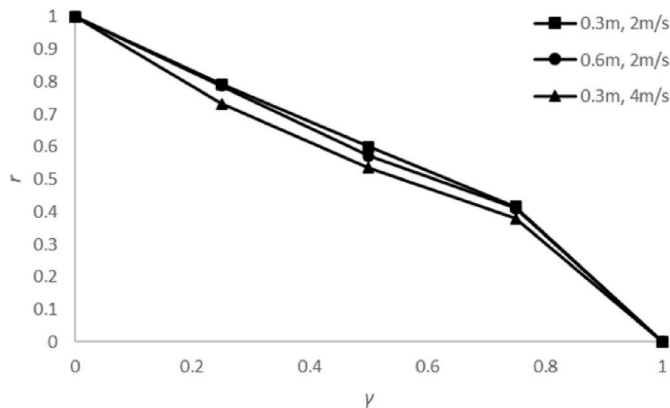


Fig. 10. Normalize ice resistance as functions of normalized channel width under different ice thickness and ship speed combinations, with Uikku as an example.

• **Type 1:** for ships with small flare angles both around the stem (the first quarter) and at the shoulder (the fourth quarter), the resistance reductions in the four quarters are relatively moderate, with no significant resistance reductions in all quarters. A typical example is Agulhas II, where all the resistance reductions are in the range of 15%–35%, which is medium. Other examples include Uikku and Polar-class icebreaker, which has larger flare angle in the fourth quarter comparing to Agulhas II, thus larger resistance reductions in the fourth quarter.

- **Type 2:** for ships with small flare angles around the stem but large flare angles at the shoulder, the resistance reductions in the fourth quarters are significant, while those in the first quarters are relatively small. In this case the resistance remains very high even the channel is largely open. A typical example is Envik, where the resistance reduction at the fourth quarter is over 55%, which is significant. Other examples include Kemira and R-class icebreaker.
- **Type 3:** for ships with large flare angles both around the stem (the first quarter) and at the shoulder (the fourth quarter), both the resistance reductions at the first quarter and at the fourth quarter are large. Examples include Tebostar and GCV. Although Tebostar has the largest mean flare angle at the fourth quarter among all the sample ships, its resistance reduction in the fourth quarter is not as high as those in the second type, because of the large resistance share in the first quarter as a result of the large flare angle around the stem.

The remaining two ships, Solano and Aranda, falls in between the three types because their hull angles around the stem and at the shoulder are medium; the resistance reductions of these two ships can be as well explained by the above reasoning. Overall, ships with large flare angles at the shoulder, e.g. Tebostar, Envik and Kemira within Type 2 and 3, endures large crushing force at the shoulder region due to the difficulty to break ice by bending, thus resulting in large remaining resistance in largely open channel. The proportion of the remaining resistance also depends on the resistance contribution from other quarters, thus ships in Type 3 demonstrates better escort performance comparing to those of Type 2. These provide a solid explanation to the different resistance-channel width curves shown in Fig. 11. Note that the escort performance does not give any indication on the icebreaking capability of a ship; it only measures the effectiveness of escort operation in narrow

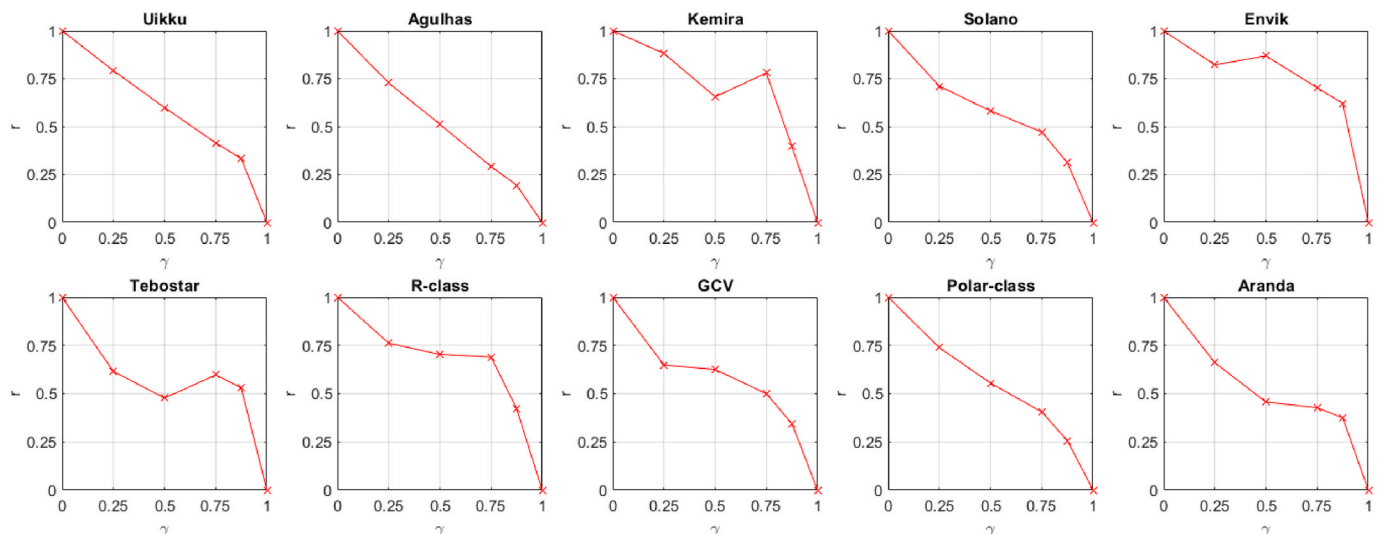


Fig. 11. Simulation results of non-dimensional resistance as functions of non-dimensional channel width.

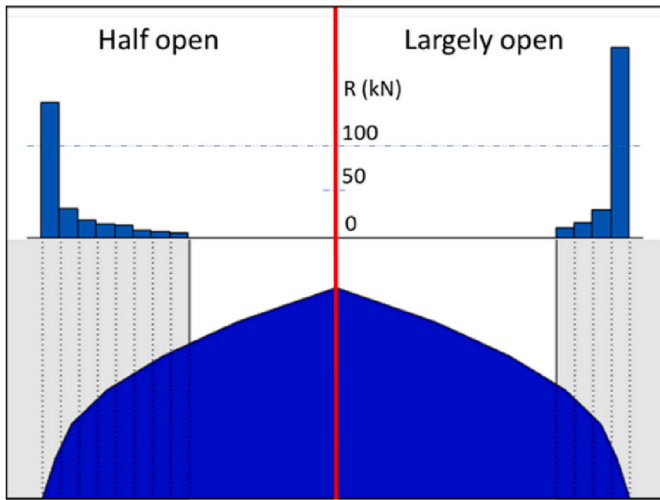


Fig. 12. Resistance distribution of Kemira along the hull in half open channel and largely open channel, ship not drawn to scale.

channel.

#### 4. Fast evaluation of ships' escort performance in a narrow channel

The above model test and numerical investigation have revealed that the resistance reduction of a ship in narrow channel depends primarily on its hull angle distribution along the waterline. For a ship with small flare angle around the stem but large flare angle at shoulder, i.e. type 2 as explained in Section 3.2, the icebreaker in front of the ship should make a wide channel so that the resistance of the escorted ship can decrease effectively. For a ship of the other types, making a channel of half the width of the escorted ship can already reduce the resistance considerably. This section aims to derive a fast method to evaluate ships' escort performance in a narrow channel based on the simulation results. Such simulation-based empirical formulae are typically derived through regression, e.g. the one by Huang et al. (2021b) for ship resistance in ice floe field. The derived method is useful when the escort performance of a ship in narrow ice channel is in question but no model scale test or numerical simulation programme are available. This is also needed in real-time decision support systems or maritime system modelling when ships' performance needs to be evaluated in short time, which is not possible with time-consuming numerical simulation.

#### 4.1. Resistance reduction in a narrow channel

According to the findings in Section 3.2, the non-dimensional resistance in a narrow channel,  $r_\gamma$ , is majorly influenced by the tangent of hull angles, here characterized with  $\varphi_1$ ,  $\varphi_2$ ,  $\varphi_3$  and  $\varphi_4$ . The aim here is to establish the function which calculates  $r_\gamma$  based on the  $\varphi$  angles of a ship. Fig. 11 has indicated strong non-linearity between  $r_\gamma$  and  $\gamma$ . For simplicity, the relationship between  $r_\gamma$  and  $r$  is set as a piecewise function segmented by  $\gamma$  equaling 0.25B, 0.5B, 0.75B, for which the simulation results are available.

The functions between  $r_\gamma$  and  $\varphi$  angles are established via linear regression using the simulation results. This gives the following regression equations:

$$r_{0.25} = 0.8048 - 0.4710 \tan \varphi_1 + 0.8421 \tan \varphi_2 - 0.6101 \tan \varphi_3 + 0.1075 \tan \varphi_4 \quad (4)$$

$$r_{0.5} = 0.6136 - 0.4700 \tan \varphi_1 + 0.7100 \tan \varphi_2 - 0.6790 \tan \varphi_3 + 0.1801 \tan \varphi_4 \quad (5)$$

$$r_{0.75} = 0.2128 - 0.4531 \tan \varphi_1 + 0.7164 \tan \varphi_2 - 0.5611 \tan \varphi_3 + 0.1990 \tan \varphi_4 \quad (6)$$

The validity of the linear regressions is demonstrated through the R-square values, which are 0.845, 0.738 and 0.879 respectively for the fitting of  $r_{0.25}$ ,  $r_{0.5}$  and  $r_{0.75}$ . The calculated  $r$  values versus simulated values are plotted in Fig. 15. All the points locate rather close to the line  $X = Y$ , indicating good fitting performance. It should be noted that the  $\varphi$  angles are not independent variables since the ship hull is smoothly curved. One should therefore not interpret the equations as the dependence of  $r$  on individual  $\varphi$  angles, which may lead to wrong conclusion such as increasing  $\varphi_3$  would decrease  $r$ .

For any channel width  $\gamma$ , the non-dimensional resistance  $r_\gamma$  can be calculated with linear interpolation between  $r_0$ ,  $r_{0.25}$ ,  $r_{0.5}$ ,  $r_{0.75}$  and  $r_1$ , noting that  $r_0$  equals 1 and  $r_1$  equals zero.

#### 4.2. Speed increment in a narrow channel

Resistance reduction is the direct influence of different channel width, while speed increment is usually the ultimate parameter of major interest for an escort operation, for which one wants to know how much gain in speed can be achieved. Typically, the  $h$ - $v$  curve of a ship in level ice is known, e.g. through model test at the design stage or theoretical calculation with existing formulae. An  $h$ - $v$  curve intercepts the ordinate by the open water speed, denoted by  $v_{ow}$ , and intercepts the abscissa by

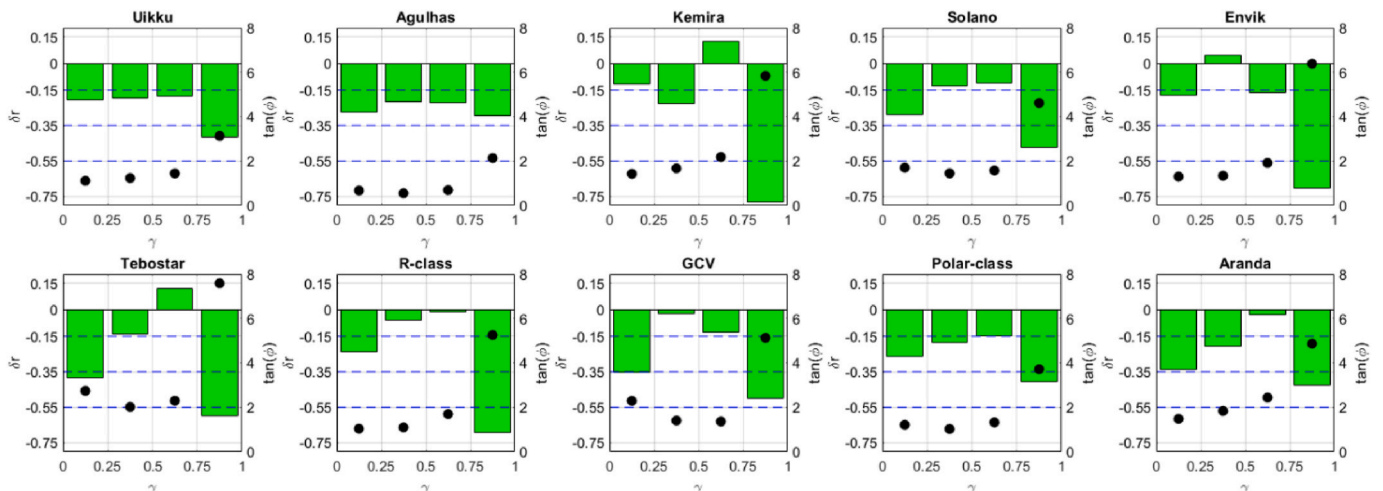


Fig. 13. Non-dimensional resistance reduction (bar charts) and tangent of the mean flare angle (scatter plots) of each ship breadth quarter.

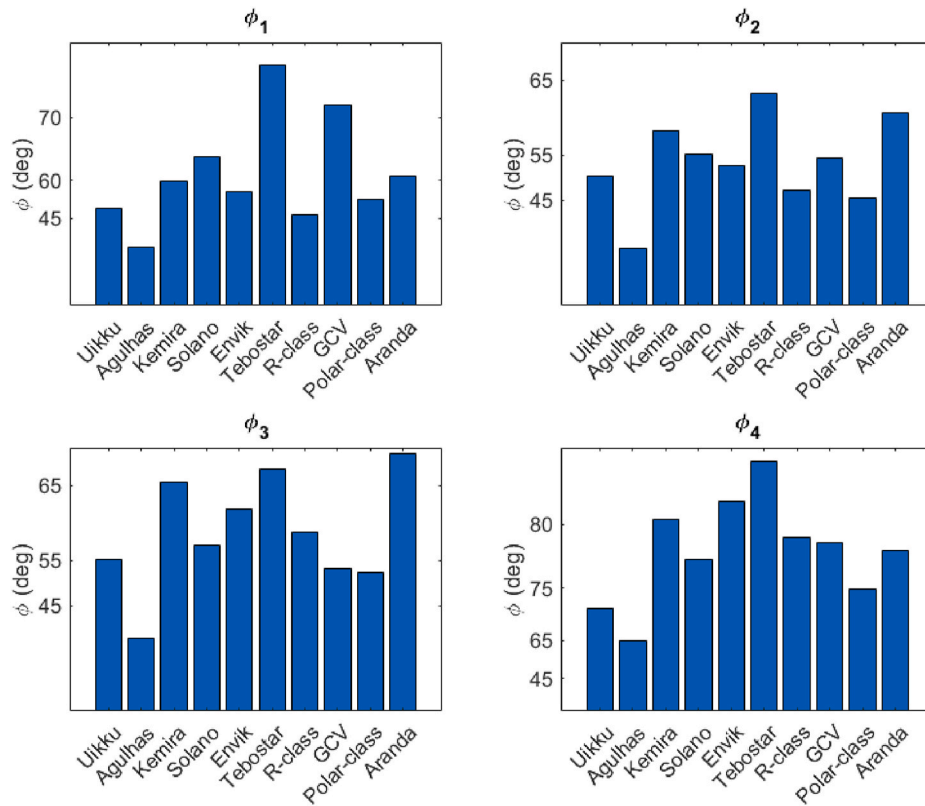


Fig. 14. Mean flare angles of the four quarters of ship width, plotted in tangent scale.

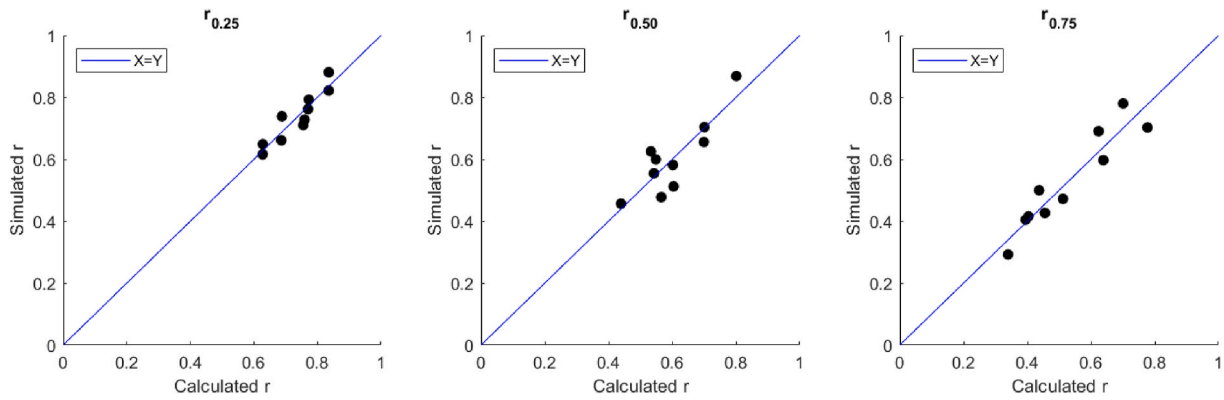


Fig. 15. Performance of linear regressions of  $\gamma_{0.25}$ ,  $\gamma_{0.5}$  and  $\gamma_{0.75}$  to the simulation results.

the maximum ice thickness which the ship can go through, denoted by  $h_m$ . Similar strategy as that for resistance-channel width curves in the previous sections can be adopted to general non-dimensional h-v curves. This is schematically shown in Fig. 16. This makes it possible to directly compare the influence of channel width on h-v curves of different ships.

The aim here is to transform an existing level ice h-v curve to narrow channel h-v curves with different channel widths. A point on an h-v curve denote the equilibrium between the propeller net thrust and ice resistance, i.e.

$$T(v_1) = R(h_1, v_1) \quad (7)$$

In a narrow channel, the resistance  $R$  is scaled by  $r_r$ , thus equilibrium established at a different thickness, i.e.

$$T(v_1) = r_r R(h'_1, v_1) \quad (8)$$

If ice resistance can be regarded as proportional to ice thickness to

the power of  $m$ , i.e.

$$R(h, v) \propto h^m \quad (9)$$

then

$$R(h'_1, v_1) = R(h_1, v_1) \left(\frac{h'_1}{h_1}\right)^m \quad (10)$$

With Eqs. (7) and (8),  $h'_1$  can be obtained as per

$$h'_1 = (\gamma_r)^{-\frac{1}{m}} h_1 \quad (11)$$

According to the level ice resistance formula of Lindqvist (1989), the three icebreaking resistance terms, namely crushing, bending and submersion resistance, are proportional to  $h^2$ ,  $h^{1.5}$  and  $h$ . Similar choice has also been indicated by other resistance formulae, e.g. the one by Riska et al. (1997) which has resistance terms proportional to  $h^2$ ,  $h^{1.5}$  and  $h$ .

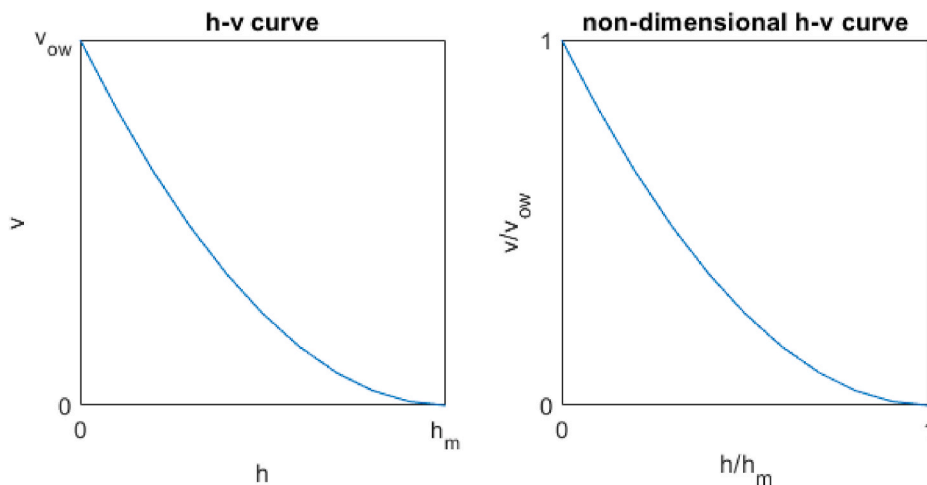


Fig. 16. A schematic h-v curve and its non-dimensionalization.

The previous version of ITTC recommendations (ITTC, 2014) mentioned that some ice tanks assume  $m$  to be 1.5 for the correction of ice resistance to the target thickness, and further mention that  $m$  is usually between 1.5 and 2. Here as a rough estimation,  $m$  is assumed to be 1.5. One can then scale an existing level ice h-v curve to a narrow channel h-v curve with a scaling factor  $(\gamma_r)^{-0.667}$ .

The non-dimensional h-v curves in narrow channels are shown in Fig. 17, with Agulhas II, Envik and GCV as examples since these are representative sample ships of the three types concluded in Section 3.2. For ships of Type 1 such as Agulhas II, increasing channel width constantly improves the escorted ship's following speed noticeably. The maximum ice thickness which Agulhas II can go through increases significantly to over two times of the level ice maximum thickness when the channel width is largely open. On the contrary, speed improvement and icebreaking capability have little improvement for ships in type 2 such as Envik, even if the channel is largely open. For ships of type 3, slight opening of the channel results in effective improvement in attainable speed and icebreaking capability, but the improvement progresses very little when the narrow channel is further opened.

## 5. Discussions

### 5.1. Implications on operational planning and ship design

The findings on h-v curves help to define effective escort strategy depending on the line drawings of a specific ship. For ships of Type 1, any increase in the channel width is effective to improve the escort performance. Therefore, it is quite likely that an assisting icebreaker narrower than the escorted ship can effectively fulfill the escorting requirement. For ships of Type 2, extensive shoulder crushing dominates the ice resistance, resulting in ineffective escort if the narrow width is less than the escorted ship. It is then better to have an assisting icebreaker which makes wider channel than the escorted ship width so that the speed of the escorted ship can be effectively improved. For ships of Type 3, a narrow channel can effectively improve ships' escort performance, but the improvement is not very sensitive to channel width, especially considering the reality that the width of icebreaker is most likely larger than 0.25 times of the escorted ship width. The width of icebreaker is then less important if the channel it creates is narrower than the escorted ship. However, if the need for a speed improvement is higher than that gained with a narrow icebreaker escort, a wider icebreaker than ship width would be needed in order to further effectively improve the escort performance.

The issue gets more complex when it comes to ship design, for which one needs to consider other factors, e.g. open water performance, level

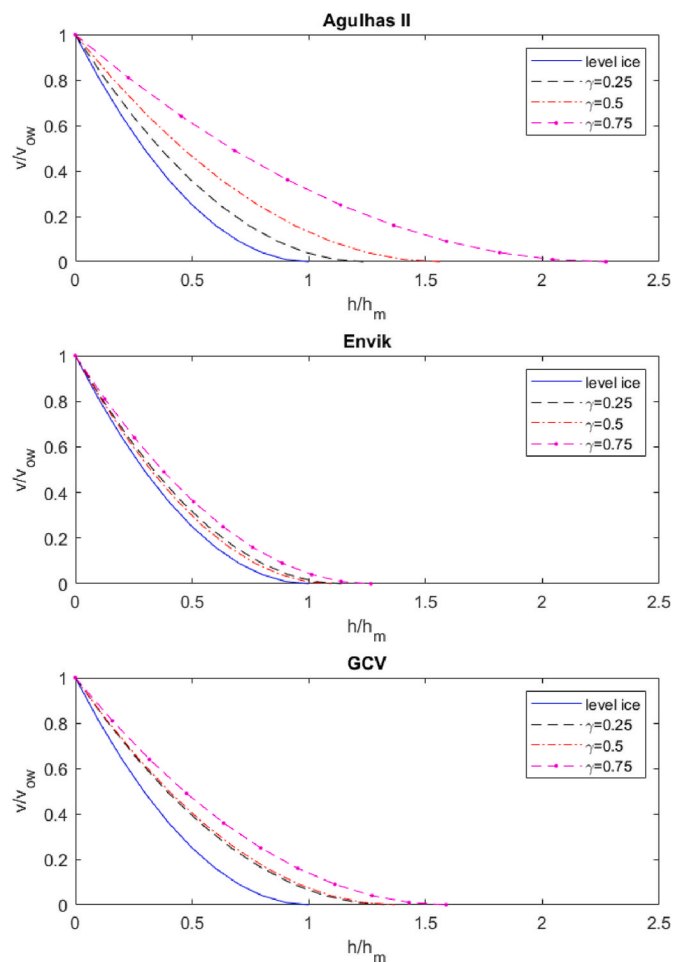


Fig. 17. Influence of channel width on h-v curves of ships.

ice performance and cargo capacity, in addition to escort performance. If a large ship having a width larger than existing icebreaker fleet is to be designed, one may consider increasing the inclination of the hull at the shoulder region, thus increasing the efficiency of icebreaker assistance. This might compromise the cargo capacity since the block coefficient will likely be reduced, therefore a balance needs to be achieved. The choice of flare angle at the stem depends on whether the ship is supposed to operate independently or to be assisted for most of the time in ice. In

the former case the stem should be more inclined while in the latter case it can be less inclined to trade for better open water performance. These are in line with typical design principles of ice-going ships.

## 5.2. Limitations and future work

The primary limitation of this work is the availability of line drawings of modern ice-going ships. Most of the ships simulated in this work are built decades ago, at which time the icebreaking performance may have been given more focus comparing to modern merchant ships which are often more optimized for open water navigation. It would be beneficial to simulate ships built in recent years to see whether their performance in a narrow channel are in line with the general conclusions obtained through this work. Another limitation comes from the assumption that submersion resistance is linearly dependent on channel width. This is a rather simplified assumption and its validity is yet to check. Recent development in numerical simulation methods coupling Discrete Element Method and Computational Fluid Dynamics (Huang et al., 2020) may offer much insight into this dependence. The third limitation comes from the model test and numerical simulation setup that the ships were towed through the channel while sway and yaw motions are restricted. In reality, the ship moves dynamically in the narrow channel where the crew maneuver the rudder to maintain the position and heading of the ship. Such dynamic process may result in some differences in the performance of ships.

## 6. Summary

This paper investigates the escort performance of ships in a narrow ice channel which has smaller width than ship width. Focuses are given to the relative change of resistance and attainable speed in comparison to those in level ice. Model tests are carried out to provide experimental insights and to benchmark the simulation programme. Numerical simulations are then implemented to further investigate the issue with ten sample ships. The investigations reveal that there are three types of ships with different features of escort performance, depending on the distribution of hull angles along the waterline. The findings are helpful for the planning of escort operation and design of merchant ships which are supposed to be escorted in ice-covered water. The obtained regression equations for the estimation of resistance reduction and transformation of  $h$ - $v$  curves are useful as fast evaluation tools for decision making.

## CRedit authorship contribution statement

**Fang Li:** Conceptualization, Methodology, Investigation, Software, Writing – original draft. **Mikko Suominen:** Investigation, Writing – review & editing. **Pentti Kujala:** Supervision, Writing – review & editing, Funding acquisition.

## Declaration of competing interest

The authors declare that they have no known competing financial interests or personal relationships that could have appeared to influence the work reported in this paper.

## Acknowledgement

The model tests have been funded by the South-eastern

Finland–Russia CBC 2014–2020 program via the project Future Potential of Inland Waterways (INFUTURE). The authors would like to thank Jarkko Toivola for the valuable discussions on the practical situation of ships in narrow ice channel.

## References

- Dobrodeev, A.A., Klementyeva, N.Y., Sazonov, K.E., 2018. Large ship motion mechanics in “narrow” ice channel. IOP Conference Series: Earth and Environmental Science. Institute of Physics Publishing, p. 12017.
- Hovilainen, M., Uuskallio, A., Romu, T., 2014. Next generation to break the ice -The oblique icebreaker. Society of Petroleum Engineers - Arctic Technology Conference 2014. Society of Petroleum Engineers (SPE), pp. 712–725.
- Huang, L., Li, M., Romu, T., Dolatshah, A., Thomas, G., 2021a. Simulation of a ship operating in an open-water ice channel. *Ships Offshore Struct.* 16, 353–362.
- Huang, L., Li, Z., Ryan, C., Ringsberg, J.W., Pena, B., Li, M., Ding, L., Thomas, G., 2021b. Ship resistance when operating in floating ice floes: derivation, validation, and application of an empirical equation. *Mar. Struct.* 79, 103057.
- Huang, L., Tuhkuri, J., Igric, B., Li, M., Stagonas, D., Toffoli, A., Cardiff, P., Thomas, G., 2020. Ship resistance when operating in floating ice floes: a combined CFD&DEM approach. *Mar. Struct.* 74, 102817.
- ITTC, 2017. Recommended procedures and guidelines.
- ITTC, 2014. ITTC – recommended procedures ITTC – test methods for model ice properties. *ReVision* 266–273.
- Kämäräinen, J., 1993. Evaluation of Ship Ice Resistance Calculation Methods (Licentiate's Thesis). Helsinki University of Technology.
- Li, F., Goerlandt, F., Kujala, P., 2020a. Numerical simulation of ship performance in level ice: a framework and a model. *Appl. Ocean Res.* 102, 102288.
- Li, F., Goerlandt, F., Kujala, P., Lehtiranta, J., Lensu, M., 2018. Evaluation of selected state-of-the-art methods for ship transit simulation in various ice conditions based on full-scale measurement. *Cold Reg. Sci. Technol.* 151, 94–108.
- Li, F., Korgesaar, M., Kujala, P., Goerlandt, F., 2020b. Finite element based meta-modeling of ship-ice interaction at shoulder and midship areas for ship performance simulation. *Mar. Struct.* 71, 102736.
- Li, F., Kotilainen, M., Goerlandt, F., Kujala, P., 2019a. An extended ice failure model to improve the fidelity of icebreaking pattern in numerical simulation of ship performance in level ice. *Ocean. Eng.* 176, 169–183.
- Li, F., Kujala, P., Montewka, J., 2019b. A ship in compressive ice: an overview and preliminary analysis. Proceedings of the 25th International Conference on Port and Ocean Engineering under Arctic Conditions. Delft, Netherland.
- Lindeberg, M., Kujala, P., Sormunen, O.V., Karjalainen, M., Toivola, J., 2018. Simulation model of the Finnish winter navigation system. *Marine Design XIII*. CRC Press, pp. 809–818.
- Lindqvist, G., 1989. A straightforward method for calculation of ice resistance of ships. Proceedings of the 10th International Conference on Port and Ocean Engineering under Arctic Conditions. Luleå, Sweden, pp. 722–735.
- Lubbad, R., Løset, S., 2011. A numerical model for real-time simulation of ship-ice interaction. *Cold Reg. Sci. Technol.* 65, 111–127.
- Matusiak, J.E., 2017. Dynamics of a Rigid Ship. Aalto University.
- Molland, A., Turnock, S., 2007. Marine rudders and control surfaces: principles, data, design and applications. *Marine Rudders and Control Surfaces*.
- Riska, K., Wilhelmson, M., Englund, K., Leiviskä, T., 1997. Performance of merchant vessels in ice in the Baltic. Research Report No. 52. Ship Laboratory, Helsinki University of Technology.
- Sazonov, K.E., 2011. Navigation challenges for large-size ships in ice conditions. *Ships Offshore Struct.* 6, 231–238.
- Su, B., Riska, K., Moan, T., 2010. A numerical method for the prediction of ship performance in level ice. *Cold Reg. Sci. Technol.* 60, 177–188.
- Suominen, M., Repin, R., Lu, L., Li, F., Kujala, P., 2021. Flexural strength of freshwater ice in Saimaa area. Proceedings of the 26th International Conference on Port and Ocean Engineering under Arctic Conditions. Moscow, Russia.
- Tan, X., Riska, K., Moan, T., 2014. Effect of dynamic bending of level ice on ship's continuous-mode icebreaking. *Cold Reg. Sci. Technol.* 106–107, 82–95.
- Wang, S., 2001. A dynamic model for breaking pattern of level ice by conical structures (Doctoral Thesis). Acta Polytech. Scand. Mech. Eng. Ser. Helsinki University of Technology.
- Zhou, L., Diao, F., Song, M., Han, Y., Ding, S., 2020. Calculation methods of icebreaking capability for a double-acting polar ship. *J. Mar. Sci. Eng.* 8, 179.